Biochemistry

 Volume 17, Number 8 April 18, 1978

Structural Changes of Ribosome by the Action of Ethylene Glycol†

J. Wesley Fox, Dennis P. Owens, and Kin-Ping Wong*,‡

ABSTRACT: The denaturation of ribosome and RNA by ethylene glycol (EG) has been studied in an attempt to further understand the conformation and stability of the ribosome. At high concentrations of EG, the ribosome, its subunits, and 16S RNA undergo drastic structural changes as shown by circular dichroism, ultraviolet absorption spectroscopy, and sedimentation velocity. Two separate conformational transitions were observed for the 30S subunit; one from 30 to 50% EG and another from 60 to 90% EG. This observation suggests the presence of two "domains" in the 30S subunit which differ in their stability. However, the 50S subunit undergoes a single sharp transition at 60 to 90% EG, consistent with the notion of a highly cooperative conformation. Association of the subunits stabilizes part of the 30S subunit since the transition curve for the 70S ribosome does not exhibit significant change at the low EG concentration region as seen for the 30S subunit. Removal of proteins from the 30S subunit broadens the transition curve to lower EG concentrations and suggests the role of proteins in stabilizing the conformation of the 16S RNA.

The solvent ethylene glycol (EG)[1] has been shown to disrupt the native structures of a number of proteins and nucleic acids (Sage & Singer, 1962; Kay & Oikawa, 1966). It is believed to preferentially disrupt hydrophobic interactions and add to the stability of hydrogen bonds. Because of this unique property, it has been used as a means of distinguishing between the contributions of these molecular interactions to the native structures of polynucleotides and nucleic acids (Fasman et al., 1964; Kay & Oikawa, 1966). In these studies and in others, the authors have concluded that hydrophobic interactions play a principal role in the stability of polynucleotides and nucleic acids (Levine et al., 1963; Ts'o & Helmkamp, 1961; Ts'o et al., 1962). The approach of many of these studies is to follow several experimental parameters which reflect structural aspects of the macromolecule and monitor the changes in these parameters upon increasing the concentration of EG. Correlating the changes observed with the denaturing effect of EG provides insight into the structure and stability of the native state and the molecular interactions responsible for maintaining the native structure.

We have examined the structural changes in the ribosome, its subunits, and 16S RNA upon the addition of 90% (v/v) ethylene glycol in the presence of a native buffer and monitored these structural changes as a function of increasing EG concentration. The results provide a further understanding of the relative structures and stabilities of the ribosome, its subunits, and 16S RNA. Furthermore, the conformational transition curves indicate, among other things, the presence of two conformational transitions in the 30S subunit, the role of ribosomal proteins in stabilizing the conformation of the RNA, and the apparent stabilization of the 30S subunit upon association with the 50S subunit.

Experimental Procedures

Ribosome, Subunits, and 16S RNA. Ribosomes were prepared from *E. coli* MRE-600 cells. The procedure followed was the $(NH_4)_2SO_4$ precipitation procedure of Kurland and coworkers (1966). Ribosomal subunits were separated by zonal ultracentrifugation (Eikenberry et al., 1970) employing a Beckman Ti-15 zonal rotor and a Model 141 gradient pump in a L5-65 preparative ultracentrifuge. Approximately 1 g of ribosomes was applied to the sucrose gradient. Displaced fractions were pooled and dialyzed exhaustively against 0.01 M Tris, 0.02 M $MgCl_2$, 0.05 M KCl (pH 7.6) to remove the sucrose. The subunits were concentrated by centrifugation, frozen in convenient aliquots, and stored at −20 °C for immediate use.

Exposure to the high concentration of $(NH_4)_2SO_4$ used in this ribosome preparation does result in a loss of 20–30% of the ribosomal proteins. However, these ribosomes have been shown to be as active for in vitro protein synthesis as crude ribosomes prepared by zonal centrifugation of bacterial extract (Kurland, 1971).

The 16S RNA used in these studies was prepared from isolated 30S subunits using the acetic acid–urea procedure of Hochkeppel et al. (1976).

Preparation of Solutions. Certified ethylene glycol obtained from Fisher Scientific Co. (E-178) was used without further purification. Stock solutions of 95% (v/v) ethylene glycol in

† From the Department of Biochemistry, University of Kansas Medical Center, Kansas City, Kansas 66103. *Received August 26, 1977.* Supported by National Institutes of Health Grant GM22962.

‡ Career Development Awardee of the National Institute of General Medical Sciences (GM 70628).

[1] Abbreviations used: EG, ethylene glycol; CD, circular dichroism.

0.01 M Tris, 0.02 M $MgCl_2$, 0.36 M KCl, pH 7.6 (95% EG-TMK_{360}), were used in all experiments. Ribosomal solutions in varying concentrations of ethylene glycol-TMK_{360} were prepared in the following manner. Initially, the 95% EG-TMK_{360} stock solution was diluted with TMK_{360} buffer in order to prepare solutions which varied in their concentration of EG. Equal volumes of these diluted EG solutions were then added to equal aliquots of starting ribosomal solutions in TMK_{360} buffer. The resulting concentration of EG in these final solutions varied from 10% to 90%, and the concentration of ribosomes, subunits, or 16S RNA was the same in each prepared solution. This method of preparation enabled a direct comparison of the ribosomal solutions containing varying amounts of EG and also ensured that a particular concentration of EG would be the same in all experiments involving the 16S, 30S, 50S, and 70S ribosomal particles, thus enabling a comparison between these four samples at varying concentrations of EG. The preparation of these ribosomal solutions was performed in a cold room at approximately 4 °C, and data were collected immediately thereafter. The starting ribosomal solutions were incubated at 40 °C for 30 min prior to the preparation of TMK_{360} and EG-TMK_{360} ribosomal solutions to ensure that the ribosomes were active.

Circular Dichroism. CD spectra were obtained with a JASCO J-20 spectropolarimeter equipped with a jacketed cell holder connected to a Lauda K2/R refrigerated temperature bath. The spectra are expressed in terms of molar ellipticity, $[\theta] = (M/dC)\theta$, where θ is the observed ellipticity in degrees, M the molecular weight, C the concentration in g/mL, and d the optical path in decimeters. The Lorentz correction factor, which relates the refractive index of the medium to the molar ellipticity observed, has not been applied here. The addition of ethylene glycol causes an increase in the refractive index which results in a decrease in molar ellipticity, after the correction has been applied. In this case, application of the Lorentz correction factor results in a small decrease in the molar ellipticity, an effect which decreases the molar ellipticities of the ribosomal particles in EG-TMK_{360} solutions further still. The spectropolarimeter was calibrated according to Cassim & Yang (1969).

Ultraviolet Absorption Spectra. Ultraviolet absorption spectra were obtained with a Cary 118 double-beam spectrophotometer equipped with water jacketed cell holders connected to a Lauda K2/R refrigerated temperature bath.

Sedimentation Velocity. Sedimentation velocity experiments were run using a Beckman Model E analytical ultracentrifuge employing schlieren optics. Ribosomal solutions were analyzed in 30-mm single sector cells at 40 000 rpm at 5 °C. The concentrations of ribosomes and subunits used in these experiments were approximately tenfold greater than the concentrations used to obtain the UV absorption and CD data. The density and viscosity of TMK_{360} and the various EG-TMK_{360} solutions were obtained at 5 °C using a pycnometer (20 mL volume) and a Cannon-Manning semimicroviscometer, respectively. In correcting the observed sedimentation coefficients to $s_{20,w}$ the following partial specific volumes for "washed" ribosomes were used: 70S ribosomes, 0.606; 50S subunits, 0.592; and 30S subunits, 0.601 (Hill et al., 1969).

Two-Dimensional Polyacrylamide Gel Electrophoresis. The procedure of Kaltschmidt & Wittmann (1970) with modifications by Knopf et al. (1975) was used.

Miscellaneous. The concentration of 70S ribosomes was measured with a Cary 118 double-beam spectrophotometer using $A_{260nm}^{1mg/mL} = 14.5$. Subunit concentrations were measured in the same manner using $A_{260nm}^{1mg/mL} = 14.5$ for the 50S subunit and $A_{260nm}^{1mg/mL} = 14.8$ for the 30S subunit. A molecular weight of 2.45×10^6 was employed for the 70S ribosome, 1.55×10^6 for the 50S subunit and 0.90×10^6 for the 30S subunit (Hill et al., 1970). The molecular weight of 2.45×10^6 for the 70S ribosome is not an experimentally determined value. Rather, it is simply the sum of the two experimentally determined values for the 30S and 50S subunits and is considered appropriate here since a good molecular weight determination has not been reported on $(NH_4)_2SO_4$ precipitated ribosomes. The concentration of 16S RNA was determined using $A_{260nm}^{1mg/mL} = 22.3$. A molecular weight of 0.64×10^6 was used for the 16S RNA (Ortega & Hill, 1973). All pH measurements were performed using a Radiometer PHM 64 research pH meter with a combined glass electrode. The water used in all experiments was double distilled and deionized.

Results

All of the results presented here were obtained at 7 °C in TMK_{360} buffer unless otherwise specified. Under these conditions no aggregation of ribosomal particles was observed as judged by high-speed centrifugation, visual inspection, and ultraviolet absorption at 340 nm.

Structural Changes at 90% (v/v) Ethylene Glycol-TMK_{360}. The conformational changes of 70S ribosome, its subunits and 16S RNA are studied by circular dichroism (CD) and ultraviolet absorption spectroscopy. Other structural changes have also been studied using sedimentation velocity experiments, including the dissociation of the ribosome into its subunits.

30S Subunit. The optical properties of the 30S subunit in TMK_{360} and in 90% EG-TMK_{360} are shown in Figure 1. The near ultraviolet CD spectrum for 30S in TMK_{360}, as shown by the solid curve in Figure 1a, is characterized by a small but distinct trough at 297 nm and a large positive peak at 265 nm. The corresponding CD spectrum for the 30S in 90% EG-TMK_{360} shows a drastic decrease in the positive peak at 265 nm from a molar ellipticity of 30×10^6 to a value of 17×10^6, and a complete disappearance of the 297-nm trough. The change in the 265 nm peak is accompanied by a red shift of 6 nm. Figure 1b shows the far ultraviolet CD spectra of 30S in TMK_{360} and 90% EG-TMK_{360}. The 30S subunit in TMK_{360} exhibits a large trough at 208 nm, which undergoes a large decrease in molar ellipticity with a concomitant red shift of 2 nm in the presence of 90% EG-TMK_{360}. The only region of the entire ultraviolet CD spectrum which is not drastically altered is the region between 220 nm and 245 nm. Here only a small increase in molar ellipticity is observed for the 90% EG-TMK_{360} state.

The ultraviolet absorption spectra for the 30S subunit under these two conditions are shown in Figure 1c. The 30S in 90% EG-TMK_{360} undergoes a hyperchromic effect with a molar absorbance increase of 3.4×10^6 M^{-1} cm^{-1} at 257 nm. Occurring along with this hyperchromic effect is a red shift of 2 nm.

50S Subunit. Figure 2a shows the near ultraviolet CD spectra of 50S subunits in TMK_{360} and in 90% EG-TMK_{360}. The changes in the spectrum due to the addition of 90% EG-TMK_{360} are similar to those observed for the 30S subunit. However, the changes are considerably less drastic. The 265-nm CD peak decreases from a molar ellipticity of 67×10^6 in TMK_{360} to 46×10^6 in 90% EG-TMK_{360}. This is a smaller percent decrease than in the case of the 30S subunit (43% for the 30S and 31% for the 50S). A less drastic change is also observed in the red shift of this peak. The peak shifts 3 nm as compared with the 6-nm red shift observed in the case of the 30S subunit. Moreover, the 297-nm trough is still clearly visible in 90% EG-TMK_{360}, although decreased and red shifted to 300 nm. The far-ultraviolet CD spectra for the 50S subunit in

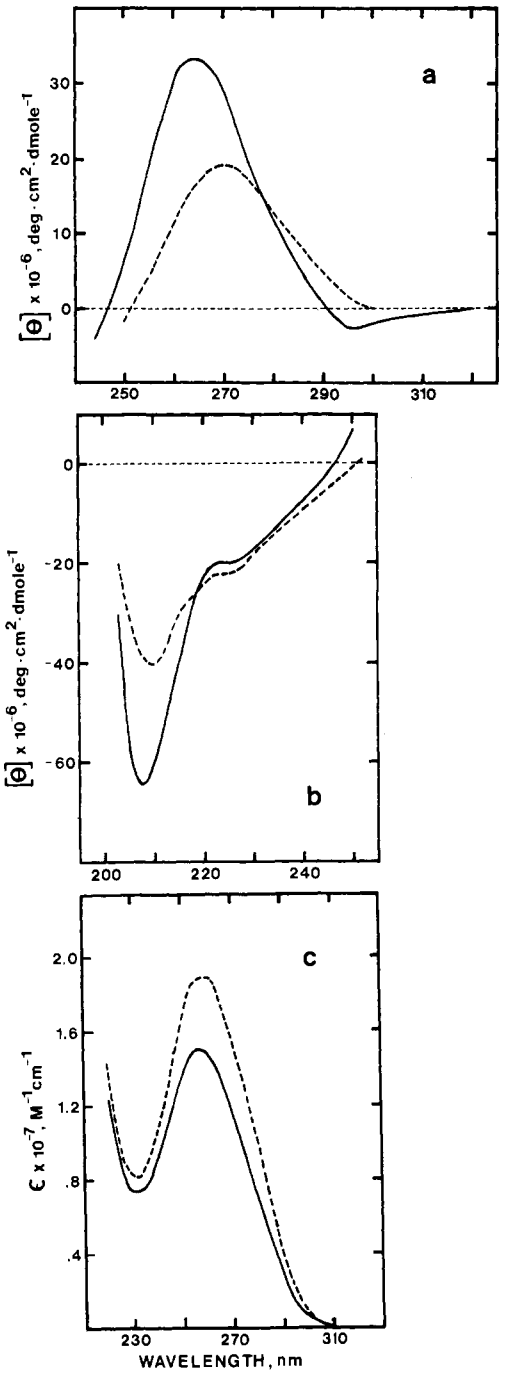

FIGURE 1: Optical properties of 30S ribosomal subunits in TMK_{360} and 90% (v/v) ethylene glycol-TMK_{360}. (a) Near-ultraviolet CD spectra; (b) far-ultraviolet CD spectra; (c) ultraviolet absorption spectra. (Solid Curves) In TMK_{360} buffer; (dashed curves) in 90% ethylene glycol-TMK_{360}. Conditions: pH 7.6, 7 ± 1 °C.

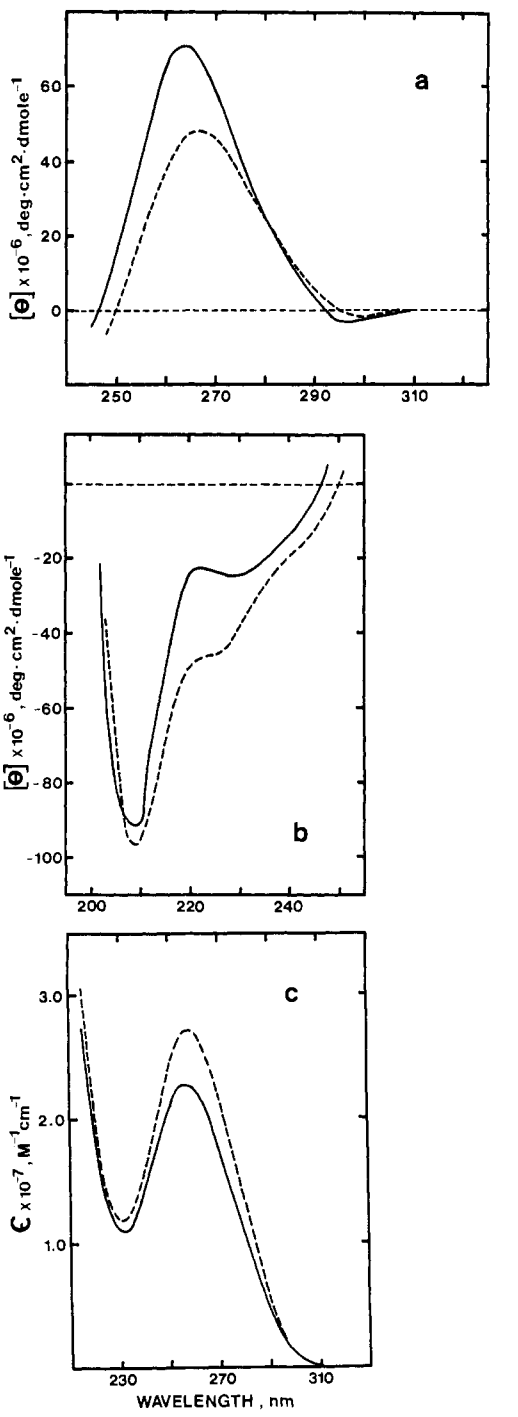

FIGURE 2: Optical properties of 50S ribosomal subunits in TMK_{360} and in 90% (v/v) ethylene glycol-TMK_{360}. Symbols and conditions are the same as Figure 1.

these two states are shown in Figure 2b, and the changes observed are quite different than in the case of the 30S subunit. The 208-nm trough in the 90% EG-TMK_{360} state exhibits a small increase in molar ellipticity, unlike the same trough in the 30S subunit which showed a large decrease. The spectral region between 220 nm and 240 nm, which showed only a small change in the 90% EG-TMK_{360} state for the 30S subunit, shows a pronounced increase in molar ellipticity for the 50S subunit.

In 90% EG-TMK_{360}, a hyperchromic effect is also observed for the 50S subunit, as was the case for the 30S subunit. Figure 2c shows that at 257 nm there is a molar absorbance increase of 4.4×10^6 M^{-1} cm^{-1}. However, the percent hyperchromicity with respect to the TMK_{360} state is less for the 50S subunit (19% for the 50S subunit and 25% for the 30S subunit). Concurrent with the hyperchromicity observed for the 50S in 90% EG-TMK_{360} is a red shift in the 257-nm absorption peak of 1 nm.

70S Ribosome. Figures 3a and 3b show the full ultraviolet CD spectra for the 70S ribosome in TMK_{360} and in 90% EG-TMK_{360}. The CD spectrum for the 70S in 90% EG-TMK_{360} resembles both the 50S and 30S subunits in the 90% EG-TMK_{360} state. The 265-nm CD peak decreases from a molar ellipticity of 102×10^6 in TMK_{360} to 66×10^6 in 90% EG-TMK_{360}, with an accompanying red shift of 3 nm. The trough at 297 nm shows a decrease in negative molar ellipticity

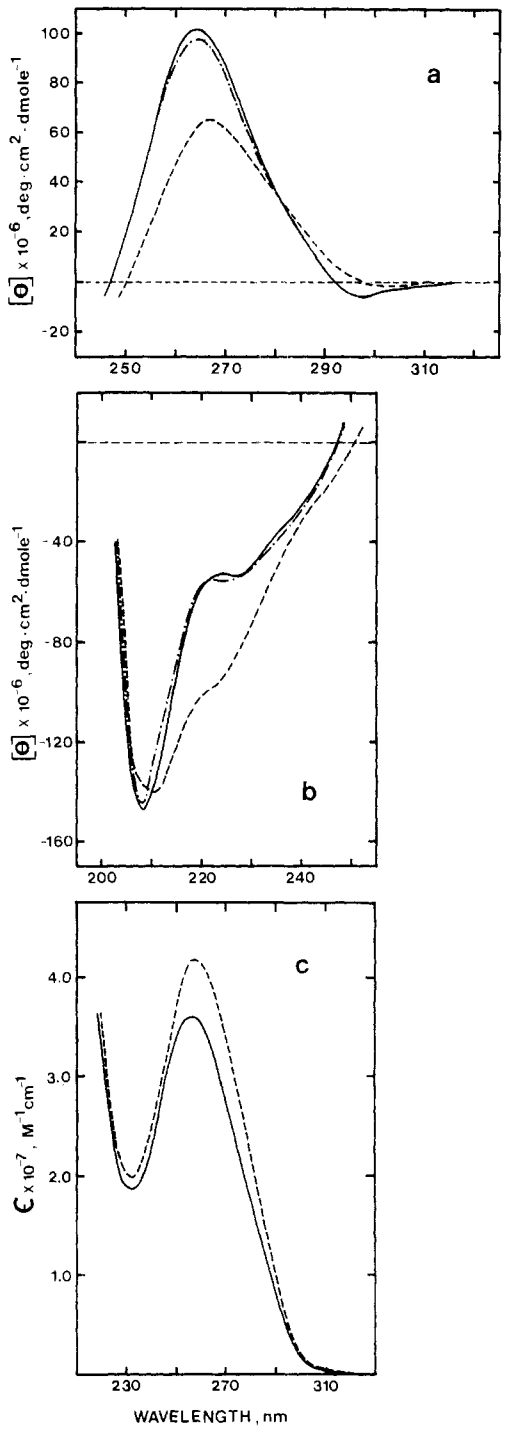

FIGURE 3: Optical properties of 70S ribosome in TMK_{360} and in 90% (v/v) ethylene glycol-TMK_{360}. Symbols and conditions are the same as Figure 1. (Broken Curve) Ultraviolet CD spectra of 70S ribosomes treated with 90% EG-TMK_{360} for 1 h at approximately 4 °C and dialyzed exhaustively against TMK_{360}.

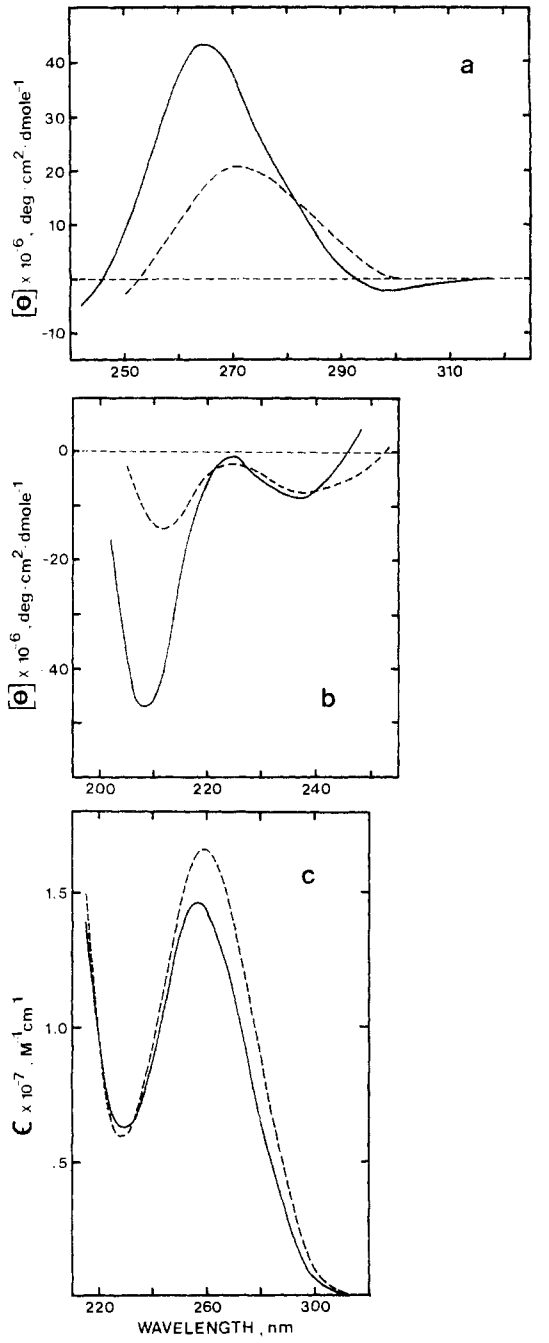

FIGURE 4: Optical properties of 16S RNA in TMK_{360} and in 90% (v/v) EG-TMK_{360}. Symbols and conditions are the same as Figure 1.

from -5.7×10^6 in TMK_{360} to -1.8×10^6 in 90% EG-TMK_{360}, along with a red shift to 303 nm. The 70S ribosome is also found to undergo a hyperchromic effect in 90% EG-TMK_{360} as shown in Figure 3c, with an increase in molar absorptivity of 5.7×10^6 M^{-1} cm^{-1} at 257 nm. Also shown in Figures 3a and 3b is the ultraviolet CD spectrum of 70S ribosomes that have been treated with 90% EG-TMK_{360} for 1 h at approximately 4 °C, followed by exhaustive dialysis against TMK_{360}. The CD spectrum indicates that treatment of the 70S ribosome with 90% EG-TMK_{360} is not totally reversible, as small differences exist between the 70S in TMK_{360} and the "treated" 70S in TMK_{360}. The "treated" 70S ribosome shows a slightly lower molar ellipticity at 265 nm and at 208 nm.

The sedimentation velocity profile of this "treated" 70S ribosome is shown in Figure 5a. The profile indicates that the original 70S ribosomes have completely dissociated, and that these subunits are sedimenting with slightly larger $s_{20,w}$ values than those determined on individual untreated subunits in TMK_{360} at 5 °C (see Table I). No change in this profile was observed after the "treated" ribosomes were heated at 40 °C for 30 min.

16S RNA. The ultraviolet CD spectra of 16S RNA in TMK_{360} and 90% EG-TMK_{360} are shown in Figures 4a and 4b. The CD spectrum is drastically altered in 90% EG-TMK_{360}, more so than in the case of the 30S, 50S, or 70S ribosomal particles. The 265-nm peak decreases from a molar ellipticity of 43×10^6 in TMK_{360} to 21×10^6 in 90% EG-

TABLE I: Corrected Sedimentation Coefficients (10^{-13} s).[a]

Sample	TMK_{360}	60% EG-TMK_{360}	90% EG-TMK_{360}
70S ribosome	70	63	
30S subunit	30	28	53
50S subunit	50	45	46

[a] Corrected sedimentation coefficients, $s_{20,w}$, for the 70S ribosome, 30S subunit, and 50S subunit in TMK_{360}, 60% EG-TMK_{360}, and 90% EG-TMK_{360}, pH 7.6, measured at 5 °C.

TMK_{360}. This is a 51% decrease and is larger than the 43% decrease observed for the 30S subunit. Also, the 265-nm peak is red shifted to 271 nm, one more nm than the red shift observed for the 30S subunit. The same is true of the cross-over points, with the 30S subunit crossing at 251 nm, and the 16S RNA crossing at 252 nm. The 208-nm trough in the far ultraviolet CD spectrum shows a large decrease in negative molar ellipticity concomitant with a red shift of 4 nm. The ultraviolet absorption spectra for 16S RNA shows an increase in molar absorptivity of 1.9×10^6 M^{-1} cm^{-1} in 90% EG-TMK_{360}, and this hyperchromic effect is accompanied by a red shift of 2 nm (see Figure 4c). This change represents a 16% increase in molar absorptivity, a value which is smaller than the 25% increase found for the 30S subunit.

Sedimentation velocity results for the 30S subunit, the 50S subunit, and the 70S ribosome in TMK_{360}, 60% EG-TMK_{360} and 90% EG-TMK_{360} are shown in Table I. The concentration of the 30S and 50S subunits in these studies was approximately 0.7 mg/mL and the concentration of the 70S ribosome was 0.9 mg/mL. The 70S ribosome and the 30S and 50S subunits were found to have corrected sedimentation coefficients, $s_{20,w}$, of 70, 30, and 50 S, respectively, in TMK_{360}. The 30S subunit sediments at $s_{20,w}$ = 28 S in 60% EG-TMK_{360}. The 50S subunit and the 70S ribosome show a somewhat larger change in their corrected sedimentation coefficients in 60% EG-TMK_{360}, with the 50S sedimenting at 45 S and the 70S sedimenting at 63 S. Figure 5b shows the sedimentation velocity profile for the 30S subunit in 90% EG-TMK_{360}. One major peak is observed sedimenting at 53 S. Such a large increase in the $s_{20,w}$ for the 30S subunit in 90% EG-TMK_{360} would suggest the formation of a dimer, but it cannot be determined from the profile whether this peak corresponds to a monomer, dimer, or some other aggregated form. In the case of the 50S subunit, the major component sediments at 46 S in 90% EG-TMK_{360}.

Conformational Transitions as a Function of Increasing EG Concentration. The conformational changes of the RNAs in the ribosomal particles, and the conformational changes of 16S RNA have been monitored by following the changes in ellipticity at 265 nm and hyperchromicity at 260 nm as a function of ethylene glycol concentration. Figure 6 shows the effect of increasing the concentration of ethylene glycol on the magnitude of ellipticity at 265 nm for the 70S ribosome and the 30S and 50S subunits. Increasing the concentration of EG generally causes a decrease in the magnitude of the $[\theta]_{265nm}$ of the ribosomal particles in TMK_{360}. Upon increasing the concentration of EG, the 30S subunit undergoes two separate conformational transitions: one occurring between 30% and 50% EG-TMK_{360} and another between 60% and 90% EG-TMK_{360}. The 50S subunit exhibits very small changes in the 265-nm peak at concentrations below 60% EG-TMK_{360}. From 60% to 90% EG-TMK_{360} the $[\theta]_{265nm}$ decreases with the largest change occurring between 80% and 90% EG-TMK_{360}. The percent $[\theta]_{265nm}$ changes for the 50S subunit are smaller

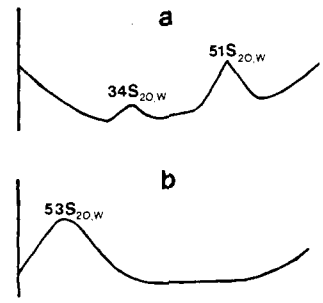

FIGURE 5: Sedimentation velocity profiles of ribosomal particles in ethylene glycol-TMK_{360}. (a) The 70S ribosome treated with 90% EG-TMK_{360} for 1 h at approximately 4 °C and dialyzed exhaustively against TMK_{360} buffer. Conditions: pH 7.6, 5 °C; rotor speed, 40 000 rpm; time, 24 min into the run; bar angle, 30°; concentration, 0.3 mg/mL. (b) The 30S subunit in 90% (v/v) ethylene glycol-TMK_{360}. Conditions: pH 7.6, 7 °C; rotor speed, 40 000 rpm; time, 100 min into the run; bar angle, 25°; concentration, 0.8 mg/mL.

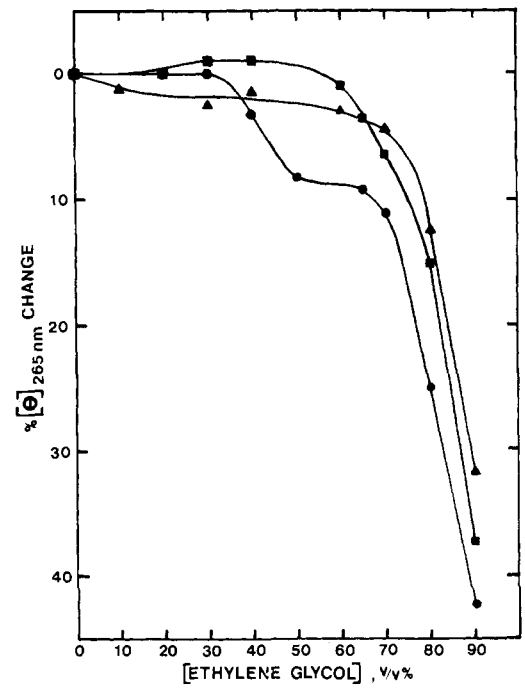

FIGURE 6: Percent molar ellipticity changes of ribosome and its subunits at 265 nm in TMK_{360} as a function of ethylene glycol concentration: (●-●) 30S subunit; (▲—▲) 50S subunit; (■—■) 70S ribosome. Conditions: pH 7.6, 7 ± 1 °C.

than the changes observed for the 30S subunit, and there is no indication of separate conformational transitions. The percent $[\theta]_{265nm}$ changes for the 70S ribosome are similar to the 50S subunit and do not appear to be the sum of the percent changes found in each of the subunits. For example, at 60% EG-TMK_{360} the percent $[\theta]_{265nm}$ change observed for the 70S ribosome is 1%, whereas the sum of the percent $[\theta]_{265nm}$ changes observed for the subunits results in a percent $[\theta]_{265nm}$ change of 4.3%. However, at 90% EG-TMK_{360} the sum of the percent $[\theta]_{265nm}$ changes for the subunits is 36%, while the percent change observed for the 70S ribosome is 37%. The similarity in these values suggests the subunits are denaturing independently and is in agreement with the above sedimentation velocity results indicating the dissociation of the 70S ribosome into its subunits in 90% EG-TMK_{360}. In the above comparisons, the percent $[\theta]_{265nm}$ change for the subunits is adjusted by multiplying the observed change by the fraction of mass contained in the subunit with respect to the whole

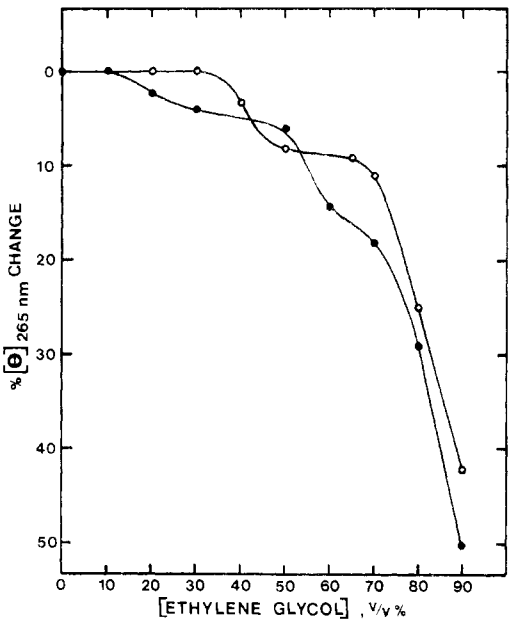

FIGURE 7: Percent molar ellipticity changes of the 30S subunit (○—○) and 16S RNA (●---●) at 265 nm in TMK_{360} as a function of ethylene glycol concentration. Conditions: pH 7.6, 7 ± 1 °C.

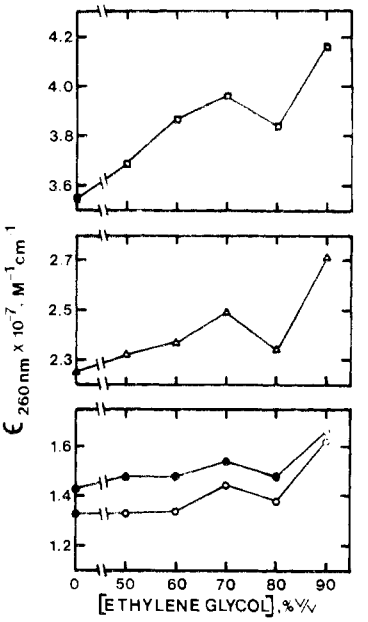

FIGURE 8: Molar absorptivity at 260 nm as a function of ethylene glycol concentration. (□) The 70S ribosome; (△) 50S subunit; (○) 30S subunit; (●) 16S RNA. Conditions: TMK_{360} buffer, pH 7.6, 7 ± 1 °C.

ribosome. This is done so the sum of the percent $[\theta]_{265nm}$ changes for the isolated subunits can be directly compared to the whole ribosome.

The changes in $[\theta]_{265nm}$ for the 30S subunit and 16S RNA are compared in Figure 7. The figure shows that 16S RNA exhibits a conformational transition in the region between 10% and 30% EG-TMK_{360}. A second transition is also apparent between 50% and 70% EG-TMK_{360} and beyond 70% EG-TMK_{360} the percent $[\theta]_{265nm}$ change continues to decrease drastically. At 90% EG-TMK_{360}, the percent $[\theta]_{265nm}$ change for the 16S RNA is 50%, the largest change observed for the ribosomal particles studied.

Changes in the molar absorptivity of the 257-nm ultraviolet absorption peak were also monitored as a function of increasing concentration of EG. Figure 8 shows the molar absorbance at 260 nm for 16S RNA, the 30S and 50S subunits and the 70S ribosome at high concentrations of EG-TMK_{360}. An increasing hyperchromic effect is seen with increasing concentration of EG for all ribosomal particles studied. An exception to this trend occurs at 80% EG-TMK_{360}, where all ribosomal particles studied exhibit a decrease in molar absorptivity, as compared with the molar absorbance at 70% and 90% EG-TMK_{360}.

Studies at Low Ionic Strength and at 25 and 37 °C. In addition to the studies performed in TMK_{360} buffer at low temperatures, similar studies of structural changes at high concentrations of EG and conformational transition curves were obtained at 25 and 37 °C, both in TMK_{360} buffer and at a lower ionic strength buffer (i.e., TMK_{50} buffer; 0.01 Tris, 0.02 M $MgCl_2$, 0.05 M KCl, pH 7.6), with essentially the same qualitative results and conclusions (Wong et al., 1976). However, various degrees of aggregation of the ribosomal particles were observed judging from high-speed ultracentrifugation (230 000*g* for 1 h), visual inspection, and absorption measurements at 340 nm.

Ribosomal Proteins Present in 90% EG-TMK_{360}. The possibility of the ribosomal particles losing some of their proteins upon treatment with 90% EG was difficult to analyze because of the very long centrifugation time involved in pelleting these particles through the viscous 90% EG-TMK_{360} solution. However, a study was performed on the 30S subunit that was treated with 90% EG at room temperature. At this temperature aggregation occurs and the ribosomal particles can be easily pelleted. Two-dimensional gel electrophoretic analysis indicates that the protein content of the "treated" 30S subunits is the same as the untreated 30S subunits, with the possible exception of one or two proteins.

Discussion

In the present study, high concentrations of ethylene glycol affect the conformation of both the RNA and protein within the ribosome. The large decrease in ellipticity and red shift of the 265-nm CD peak, as observed at 90% EG-TMK_{360} for the ribosomal particles and 16S RNA, are alleged to originate from the breakdown of the RNA's conformation (Vournakis & Scheraga, 1966; Yang & Sameijima, 1969; Brahms & Mommaerts, 1964). The changes observed in this near ultraviolet region of the CD spectrum (250–320 nm) are due solely to the ribosomal RNA, since the proteins do not contribute to the observed CD at these wavelengths. The hyperchromicity observed in the ultraviolet absorption spectra for each of the four particles at 90% EG-TMK_{360} also suggests that the secondary structure of the RNA has been disrupted. The far ultraviolet CD spectrum for ribosome is made up of contributions from both the RNA and protein in the ribosome. However, the region around 222 nm probably reflects contributions mainly from the α-helical structure of the proteins, since ribosomal RNA normally has zero or negligible ellipticity around 222 nm.

It is apparent from these studies that the 30S and 50S subunits respond differently to 90% EG-TMK_{360}, both with respect to their RNA and protein components. The conformation of the RNA within the 50S subunit is disrupted to a lesser extent than the 16S RNA within the 30S subunit and, thus, indicates its greater stability with respect to the denaturing effects of ethylene glycol. The proteins of the 50S subunit, however, seem to be affected to a greater extent than the proteins of the 30S subunit. The 30S subunit shows small changes in the 222-nm region of the CD spectrum at 90% EG-TMK_{360}. However, the 50S subunit shows a drastic increase in molar

ellipticity in this region, and it is apparent that the proteins in the two subunits are affected differently by the addition of 90% EG–TMK_{360}. A possible explanation for this difference could lie in the nature of the proteins within each ribosomal subunit. A comparison of amino acid composition data on the 30S and 50S subunits of *E. coli* ribosome (Kaltschmidt et al., 1970) reveals that the proteins from the 50S subunit are more hydrophobic in nature. Of the 50S ribosomal proteins examined, 20 of them have a ratio of nonpolar to polar amino acids greater than one, and 8 have a ratio less than one. In the 30S subunit, 6 proteins have a nonpolar to polar ratio greater than one, while 13 have a ratio less than one. Moreover, the 50S subunit contains 6 proteins with distinctively high amounts of nonpolar residues (approximately 58%), whereas the 30S subunit contains only 2 proteins with this larger amount of nonpolar residues. The greater amount of hydrophobic residues in the 50S subunit proteins might cause these proteins to be affected to a greater extent by the hydrophobic-disruptive reagent ethylene glycol. Instead of the proteins unfolding to random coils, a possible conformation which might be induced is an α-helical structure. In this conformation, the hydrophobic residues would be exposed to the solvent, while hydrogen bonds would form between the peptides groups within the helix. This possibility has been suggested by Nozaki & Tanford (1965) making use of calculations on the free energy of unfolding of β-lactoglobulin based on solubilities of amino acids and peptides in aqueous ethylene glycol. Their data show that ethylene glycol causes a reduction in the free energy of hydrophobic interactions between nonpolar groups and water, but increases the free energy of contact between peptide groups and the solvent. Experimental results have shown that ethylene glycol does cause a sharp rise in the $-b_0$ parameter obtained from optical rotatory dispersion of β-lactoglobulin (Tanford et al., 1962) suggesting an increase in the α-helical content of this protein. An increase in the helical content of the ribosomal proteins would indeed explain the large increase at 222 nm exhibited by the 50S subunit in 90% EG–TMK_{360}.

The structural changes caused by the addition of 90% EG seem to be for the most part reversible, as only small differences are present in the CD spectrum of the "treated" ribosome, and the $s_{20,w}$ of the subunits (see Figure 5). However, the small structural changes observed seem to be enough to affect the ability of the subunits to reassociate, as the presence of Mg(II) and other salts is not sufficient to cause these subunits to reassociate. Also, incubating the "treated" ribosomes at 40 °C for 30 min did not affect the dissociated state of these ribosomes. Untreated isolated subunits were found to reassociate in TMK_{360} (unpublished results). These results suggest that the ribosome is irreversibly dissociated into its subunits upon treatment with 90% EG.

The sedimentation velocity data summarized in Table I indicate that at 90% EG–TMK_{360} the 50S subunit retains its overall native shape to a greater extent than the 30S subunit. However, it should be pointed out that it is impossible to determine conclusively whether the major peak sedimenting at 53 S is a monomer, a dimer, or some other aggregated form of the 30S subunit. At 60% EG–TMK_{360}, the 70S ribosome seems to be affected to the same degree as the 50S subunit. At 90% EG–TMK_{360}, however, it appears that the 70S ribosome is completely dissociated into its subunits, as noted above. It should be mentioned that the corrected sedimentation coefficients for the ribosomal particles in EG are subject to some uncertainty as a result of a probable change in the partial specific volume in EG.

The 265-nm CD peak present in ribosome and ribosomal RNA arises from the induced asymmetric environment of the bases in the RNA in the form of base stacking and base pairing and is a measure of the overall conformation of the RNA as it exists in the ribosome or free in solution. Following this parameter as a function of increasing EG concentration enables a measure of the effect that the hydrophobic solvent EG has on the conformation of the RNA. Increasing concentrations of EG result in conformational changes in the RNA. In the 30S subunit, increasing the concentration of EG results in two separate conformational transitions. The results suggest the presence of two "domains" having different stabilities in the 30S subunit. The presence of two separate structural regions in the 30S subunit has been observed using electron microscopy (Wabl et al., 1973; Lake, 1976; Tischendorf et al., 1974, 1975). It is likely that the two domains of the 30S subunit inferred from this study correspond to the two physically separate structural regions observed in electron micrographs. In addition, the present study suggests that they have significantly different stabilities in undergoing conformational transitions. The conformational transition curve for 16S RNA indicates that these two stability domains are also present in isolated 16S RNA.

Throughout the higher concentrations of EG–TMK_{360}, the 50S subunit exhibits smaller changes in the $[\theta]_{265nm}$ than the 30S subunit. These smaller changes indicate that the conformation of ribosomal RNA within the 50S subunit is more stable to the denaturing effects of EG. This was also indicated by the ultraviolet absorption and CD spectra of the subunits in TMK_{360} and 90% EG–TMK_{360}. Also apparent from the data in Figure 5 is the stabilization of the 30S subunit upon association with the 50S subunit. At 60% EG–TMK_{360}, the sum of the percent $[\theta]_{265nm}$ changes for the 30S and 50S subunits (after a correction has been made enabling a direct comparison with the 70S ribosome) is larger than the percent $[\theta]_{265nm}$ change observed for the 70S ribosome. The increase is largely associated with the 30S subunit and suggests that this subunit is more stable to the disrupting effects of EG when associated with the 50S subunit. This change in stability presumably results from a conformational change in the 30S subunit upon dissociation from the ribosome. Enzymatic iodination studies (Litman et al., 1974) have indicated that many of the 30S proteins within the 30S subunit undergo a conformational change upon formation of the 70S ribosome. Teraoka & Tanaka (1972) have studied the binding of dihydrostreptomycin to the 30S subunit and have concluded that association of the 30S subunit with the 50S subunit induces an alteration in the conformation of the 30S subunit and a consequent change in its ability to bind dihydrostreptomycin.

The conformational transition curves shown in Figure 7 indicate that the binding of the proteins aids in stabilizing the 16S RNA against the action of EG. At the various concentrations of EG–TMK_{360}, a larger percent $[\theta]_{265nm}$ change is observed for the 16S RNA, indicating a greater amount of its conformation has been disrupted. This transition profile is similar to that observed by Kay & Oikawa (1966) for wheat germ tRNA. In this study the authors concluded that hydrophobic forces play a principal role in maintaining the native structure of tRNA. This conclusion is based on the preferential effect of EG to disrupt hydrophobic bonds, and the observation of a collapse in the native structure of wheat germ tRNA upon the addition of EG. In agreement with this conclusion is the recent high resolution x-ray diffraction structure of yeast $tRNA^{Phe}$ indicating base stacking as the major stabilizing feature of the molecule (Quigley & Rich, 1976). The similarity in the two transition curves indicates this same conclusion can be applied to 16S RNA; i.e., the role of hydrophobic forces in stabilizing the native structure of 16S RNA.

The hyperchromic effects shown in Figure 8 for the ribosomal particles and 16S RNA correlate well with the observed CD changes at high concentrations of EG-TMK_{360}. Both changes indicate the disruption of secondary structure in the RNA. However, there is one concentration of EG-TMK_{360} which is a consistent exception to the hyperchromic effects observed at high concentrations of EG-TMK_{360}. This occurs at 80% EG-TMK_{360}, and at this particular concentration of EG, a decrease in the molar absorbance is seen for each of the particles studied. This result is quite unexpected, but an explanation dealing with an increasing amount of electrostatic contribution to the free energy of stabilization seems reasonable. EG is a solvent of high polarizability and low dielectric constant, and in such a solvent the stabilization due to electrostatic contributions could compensate for the loss of stacking forces due to ethylene glycol's disrupting effect on these hydrophobic forces (Hanlon & Major, 1968; Green & Mahler, 1970). At a particular concentration of EG-TMK_{360}, this stabilization could permit more interactions between the bases and result in a decrease in the molar absorptivity. The decrease in molar absorbance need not be accompanied by an increase in molar ellipticity, as these two parameters are not sensitive to the same structural features and are therefore not necessarily complementary (Rosenfeld, 1928; Cox & Littauer, 1960; Davis & Tinoco, 1968). Hypochromicity is sensitive to the stacking and pairing of base chromophores and relatively insensitive to the precise geometry, whereas circular dichroism measures the rotatory strength of the chromophore and is sensitive to the geometries of the component transition dipoles.

References

Brahms, J., & Mommaerts, W. F. H. M. (1964) *J. Mol. Biol. 10*, 73-88.

Cassim, J. Y., & Yang, J. T. (1969) *Biochemistry 8*, 1947-1951.

Cox, R. A., & Littauer, U. Z. (1960) *J. Mol. Biol. 2*, 166-168.

Davis, R. C., & Tinoco, I. (1968) *Biopolymers 6*, 223-242.

Eikenberry, E. F., Bickle, T. A., Traut, R. R., & Price, C. A. (1970) *Eur. J. Biochem. 12*, 113-116.

Fasman, G. D., Lindblow, C., & Grossman, L. (1964) *Biochemistry 3*, 1015-1020.

Green, G., & Mahler, H. R. (1970) *Biochemistry 9*, 368-387.

Hanlon, S., & Major, E. O. (1968) *Biochemistry 7*, 4350-4358.

Hill, W. E., Anderegg, J. W., & Van Holde, K. E. (1969) *J. Mol. Biol. 44*, 263-277.

Hill, W. E., Anderegg, J. W., & Van Holde, K. E. (1970) *J. Mol. Biol. 53*, 107-121.

Hochkeppel, H.-K., Spicer, E., & Craven, G. R. (1976) *J. Mol. Biol. 101*, 155-170.

Kaltschmidt, E., Dzionara, M., & Wittmann, H. G. (1970) *Mol. Gen. Genet. 109*, 292-297.

Kaltschmidt, E., & Wittmann, H. G. (1970) *Anal. Biochem. 36*, 401-412.

Kay, C. M., & Oikawa, K. (1966) *Biochemistry 5*, 213-223.

Knopf, U. C., Sommer, A., Kenny, J., & Traut, R. R. (1975) *Mol. Biol. Rep. 2*, 35-40.

Kurland, C. G. (1971) *Methods Enzymol. 20*, 379.

Kurland, C. G. (1966) *J. Mol. Biol. 18*, 90-108.

Lake, J. A. (1976) *J. Mol. Biol. 105*, 131-159.

Levine, L., Gordon, J. A., & Jencks, W. P. (1963) *Biochemistry 2*, 168-175.

Litman, D. J., Lee, C. C., & Cantor, C. R. (1974) *FEBS Lett. 47*, 268-271.

Nozaki, Y., & Tanford, C. (1965) *J. Biol. Chem. 240*, 3568-3573.

Ortega, J. P., & Hill, W. E. (1973) *Biochemistry 12*, 3241-3243.

Quigley, G. J., & Rich, A. (1976) *Science 194*, 796-806.

Rosenfeld, L. (1928) *Z. Phys. 52*, 161.

Sage, H. J., & Singer, S. J. (1962) *Biochemistry 1*, 305-317.

Tanford, C., Buckley, III, C. E., De, P. K., & Lively, E. P. (1962) *J. Biol. Chem. 237*, 1168-1171.

Teraoka, H., & Tanaka, K. (1972) *Biochem. Biophys. Res. Commun. 46*, 93-98.

Tischendorf, G. W., Zeichhardt, H., & Stoffler, G. (1974) *Mol. Gen. Genet. 134*, 209-223.

Tischendorf, G. W., Zeichhardt, H., & Stöffler, G. (1975) *Proc. Natl. Acad. Sci. U.S.A. 72*, 4820-4824.

Ts'o, P. O. P., & Helmkamp, G. K. (1961) *Tetrahedron 13*, 198.

Ts'o, P. O. P., Helmkamp, G. K., & Sander, C. (1962) *Biochim. Biophys. Acta 55*, 584-600.

Vournakis, J. N., & Scheraga, H. A. (1966) *Biochemistry 5*, 2997-3006.

Wabl, M. R., Barends, P. J., & Nanninga, N. (1973) *Cytobiologie 7*, 1.

Wong, K.-P., Fox, J. W., & Owens, D. P. (1976), Abstracts, 10th International Congress Biochemistry, Hamburg, West Germany, p 113.

Yang, J. T., & Sameijima, T. (1969) *Prog. Nucleic Acid Res. Mol. Biol. 9*, 223-300.